Investigation of index of refraction changes in chalcogenide glasses during molding processes.

Jacklyn Novak[1], Ray Pini[1], William V. Moreshead[1], Erik Stover[2], Alan Symmons[1]
[1]LightPath Technologies, Inc., 2603 Challenger Tech Ct, Ste 100, Orlando, FL, USA 32826
[2]M[3] Measurement Solutions, Inc., 2048 Aldergrove Ave, Suite D, Escondido, CA 92029

ABSTRACT

Precision glass molding has a well-documented effect of a decrease in the index of refraction of the glass during the molding process. This index drop has such significant value that optical designs for molded lenses must take into account the index drop to accurately determine the optical performance of the final lens. Widespread adoption of chalcogenide glasses for molded infrared optics has raised a series of questions as to the behavior of these glasses under molding conditions. This paper will investigate the index of refraction changes in two different chalcogenide glasses and determine if these changes are significant enough for optical designers to consider in their designs.

Keywords: Precision glass molding, chalcogenide glass, refractive index, infrared

1. INTRODUCTION

Until recently, the only materials used for infrared optics were salts and crystals such as germanium or zinc selenide. These materials require expensive processing techniques and the materials themselves also have a high cost. Chalcogenide glasses (ChGs) were invented to meet the increasing demand for low-cost infrared optics. Examples of ChGs include $Ge_{28}Sb_{12}Se_{60}$ and $As_{40}Se_{60}$. These materials are less expensive due to containing little to no germanium. Processing costs are also reduced because ChGs are moldable.

Precision glass molding (PGM) is an alternative to traditional methods of producing high quality optical lenses. In PGM, a glass preform is placed between optical quality molds, heated to the molding temperature, pressed, and then cooled. Figure 1 shows an assortment of IR lenses molded from chalcogenide glass. For high volume production, PGM is superior to the traditional methods. PGM offers increased efficiency because the molding cycle is much shorter than the process of grinding and polishing or diamond turning a lens. Production costs are also decreased because the molds can be reused for pressing many lenses.

Figure 1 – Molded chalcogenide glass lenses

Material properties are important in lens design and must be taken into account along with the shape accuracy and surface finish. The glass is heated above its glass transition temperature (T_g) during the PGM process, so the thermal history of the glass is altered and can therefore change the glass properties. These changes must be well understood and taken into account in the lens design in order to maximize the optical performance of the lens. The cooling rate is of

Electro-Optical and Infrared Systems: Technology and Applications X, edited by David A. Huckridge, Reinhard Ebert,
Proc. of SPIE Vol. 8896, 889602 · © 2013 SPIE · CCC code: 0277-786X/13/$18 · doi: 10.1117/12.2028902

particular importance, as the glass is cooled much faster after molding than after annealing. Typically a decrease in refractive index is measured for oxide glasses, and this "index drop" is a well-documented effect of the fast cooling rate during molding [1-2], but this effect remains largely unstudied in chalcogenide glass. In oxide glasses, it has been shown that the refractive index variation is smaller at longer wavelengths [2]. Chalcogenide glasses are used for applications at long wavelengths, but the chemical make-up is quite different from oxide glasses so they must be investigated to see if the index is significantly changed after molding.

The purpose of this paper is to study the effect of PGM on the refractive index of chalcogenide glasses. Previous studies on oxide glasses assumed that the refractive index drop was dependent only on the cooling rate and the experiments were performed without compression of the glass [2-3]. The same assumption was used here. Index measurements were made on polished round diameter wedges of chalcogenide glasses both before and after subjecting them to thermal cycles which could mimic the PGM process. Two different cooling rates were studied in order to determine what changes occur and if they are significant enough for optical designers to consider in their designs.

2. EXPERIMENT

Glass Molding Process

Two chalcogenide glasses, $Ge_{28}Sb_{12}Se_{60}$ and $As_{40}Se_{60}$, were studied in these experiments. Samples of these glasses were machined into round diameter wedges with polished faces.

This research focused only on the effect of the cooling rate on the refractive index. The samples were placed on an optical quality mold in a precision glass molding machine. They were then subjected to a thermal cycle mimicking that of a molding process, but no pressure was applied. The thermal profiles are shown in Figure 2 below. Two cooling rates, 5°C/min ("fast") and 2°C/min ("slow"), were compared. These rates are much faster than the cooling rate following the annealing of the glass boules, which is typically 2°C/hr.

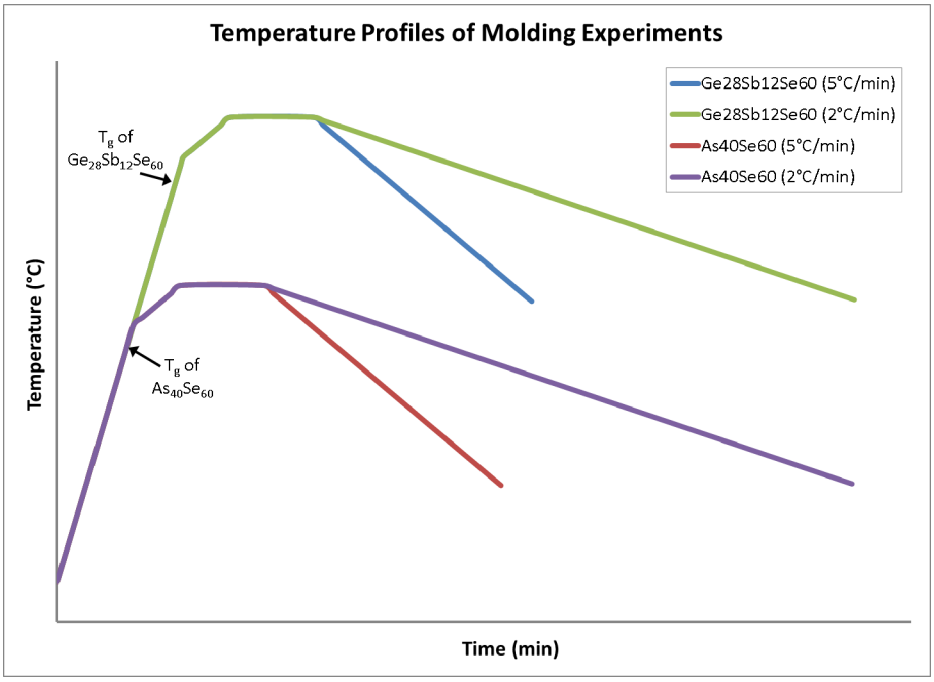

Figure 2: Temperature Profiles of Molding Experiments

Four samples were tested for each glass type – 2 with the fast cooling rate and 2 with the slow cooling rate. They were heated to a molding temperature, $T_{mold,}$ above the glass transition temperature (T_g) of the glass. Then they were held at that temperature for 10±2 minutes before cooling. The T_g's of $Ge_{28}Sb_{12}Se_{60}$ and $As_{40}Se_{60}$ are approximately 285°C and 185°C, respectively.

The flatness was measured again following the heat treatments to ensure that the surfaces were still adequate for index measurements. While the surfaces of the samples were affected somewhat by the heat treatments, refractive index measurements were still possible on the majority of the samples. The change in index was evaluated following final refractive index measurements.

Refractive Index Measurements

Refractive index measurements were made by M^3 Measurement Systems, Inc. using a modified minimum deviation technique. The M^3 refractometer is an automated refractive index test station with automation controlled by internally developed LabView software.

The basic operation utilizes the collimated output of a broad-band monochromator to select the wavelengths of interest. An aluminum off-axis parabolic (OAP) mirror is used to collimate the output beam of an F/4 monochromator. The collimated beam enters the sample at a known incident angle, which can be adjusted by rotating the position of the sample with a precision encoded rotation stage. The incident angle is calculated to set the sample at the minimum deviation angle based on a pre-entered estimate of the refractive index. This is done so the sweep function of the detector assembly can find the refracted beam quickly.

An image of the monochromator exit slit is formed at the detector slit after passing through the sample. Measurement of the refracted beam angle is done by sweeping the detector assembly across the image in three iterations. The first iteration sweeps quickly through a large angle, generally 8-20°, depending on how well known the material's refractive index is. The sweep is centered on the calculated refracted angle. Once the sweep is finished, the peak position of the line spread function is calculated. The second iteration sweeps at a moderate speed through 1-2° centered on the measurement from the first iteration. The third iteration then steps across the image at a slow speed through 0.25-0.5° to obtain high resolution data logging of the image. The curve-fit peak position of the line spread function is calculated to yield the refracted angle.

The values for refracted angle, wavelength, apex angle, temperature, and incident angle are recorded and used to calculate the refractive index. Multiple averages are taken to help reduce uncertainty. For traceability, a CaF_2 prism previously measured at the National Institute of Standards and Technology (NIST) and a ZnS (multi-spectral) prism from the German national lab PTB are used to calibrate the system. The PTB sample is a traceable standard certified to $\pm 2 \times 10^{-6}$.

This system is a modified re-creation of a system originally designed at the Optical Science Center at the University of Arizona by B.C. Platt and later adapted by James Palmer.

This technique can yield results accurate to the 4th decimal place at room temperature if the wedge samples have sufficiently flat surfaces. The flatness of the samples was measured using a FISBA OPTIK interferometer prior to index measurement to ensure they were adequate. The index was measured at 20°C in air at 2, 4, 6, 8, 10, and 12μm.

3. RESULTS & DISCUSSION

The refractive index of each wedge was measured at 2, 4, 6, 8, 10 and 12μm before and after the molding cycle experiments. The dispersion curves for the $Ge_{28}Sb_{12}Se_{60}$ samples are plotted in Figure 3. A single averaged curve is shown for the 4 samples as-annealed (before heat treatment), as well as for the 2 samples that were cooled at 5°C/min following the heat treatment. Unfortunately, the 2 samples cooled at 2°C/min no longer had sufficiently flat surfaces after the heat treatments and index measurements could not be obtained.

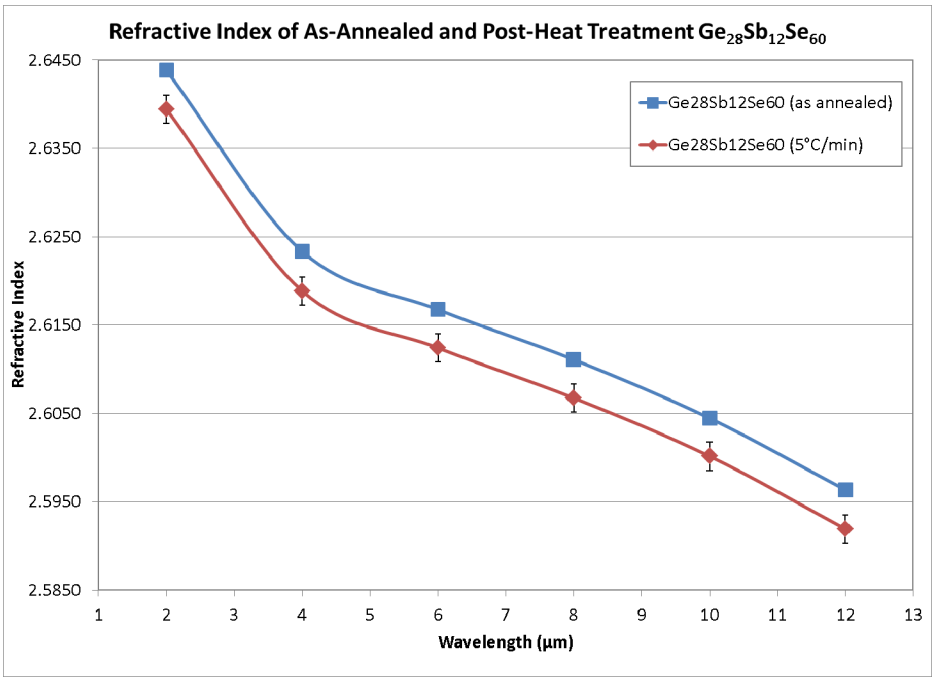

Figure 3: Dispersion curves of $Ge_{28}Sb_{12}Se_{60}$ samples before and after heat treatments

The error bars for the as-annealed index values are within the size of the data points. The error in the measurements after heat treatment is due in part to the poor surface flatness, but more samples would need to be tested to determine if there is in fact some part-to-part variation.

The $As_{40}Se_{60}$ samples were treated in the same way as the $Ge_{28}Sb_{12}Se_{60}$ samples, except with a lower value of T_{mold}. The dispersion curves are shown in Figure 4. Index measurements were obtainable from all 4 of the samples.

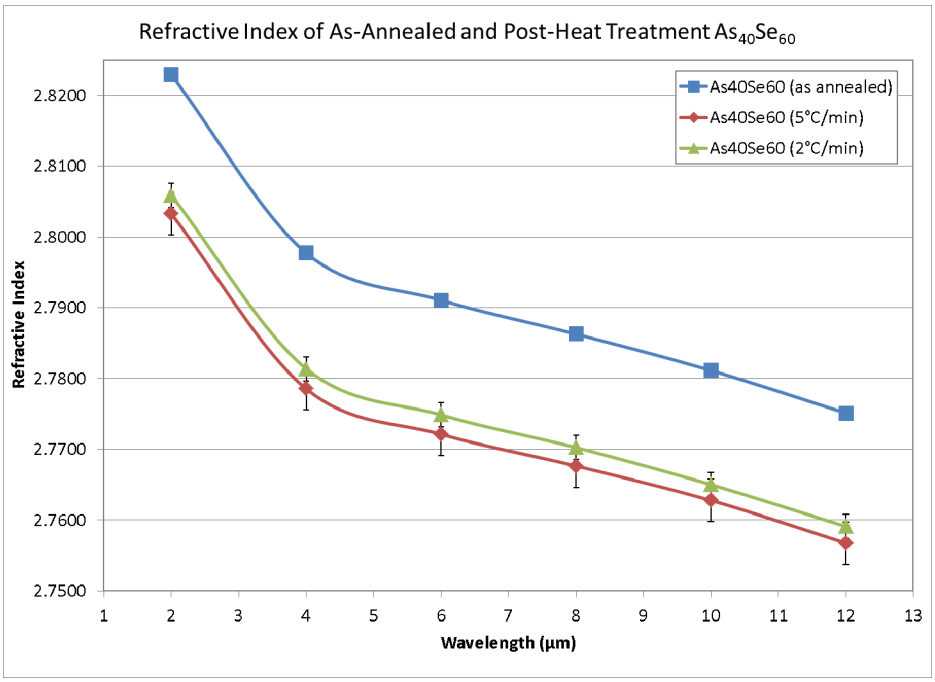

Figure 4: Dispersion curves of $As_{40}Se_{60}$ samples before and after heat treatment

As with the $Ge_{28}Sb_{12}Se_{60}$ samples, the error bars for the as-annealed index values are within the size of the data points. The error in the measurements after heat treatment is again due in part to the poor surface flatness, but more samples would need to be tested to determine if there is in fact some part-to-part variation. With these samples, there is data for two heating rates that can be compared. The data shows that the faster the cooling rate is, the lower the index of the sample is. The index decreases from the as-annealed (cooled at 2°C/hr) samples to the samples cooled at 2°C/min and the samples cooled at 5°C/min have the lowest index. However, the values for the two faster cooling rates are within error, and more samples should be tested to determine if the difference in index due to the difference in cooling rates is, in fact, statistically significant..

The difference between the as-annealed index and the post-heat treatment index was calculated for each sample and will be referred to as the index drop. The results for both $Ge_{28}Sb_{12}Se_{60}$ and $As_{40}Se_{60}$ are plotted in Figure 5 below.

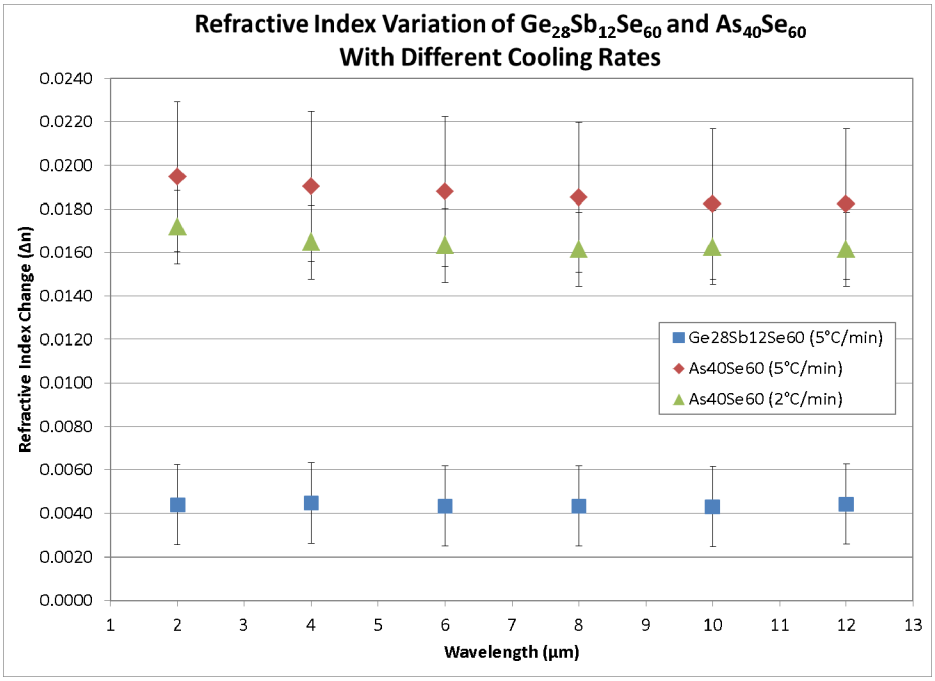

Figure 5: Index drop after heat treatment of $Ge_{28}Sb_{12}Se_{60}$ and $As_{40}Se_{60}$ samples

As seen in the figure, the index drop for the $As_{40}Se_{60}$ samples is significantly larger than the index drop seen in $Ge_{28}Sb_{12}Se_{60}$. This means that the index drop will play a larger role in the design of lenses made from the $As_{40}Se_{60}$ material.

With these index drop values, we explored the effect of the index drop on example lenses. From LightPath's catalog, the first lens we checked was a 7.7 mm, f1.2 thermal imaging lens as shown in figure 6. If we substitute the post molding index of refraction and maintain the same distance from the lens to the image plane, the focal plane of the lens is shifted 0.002 mm away from the lens and the MTF drops by 8%. A simple refocusing brings the MTF back to the initial values. The amount of focal shift at this level is within the manufacturing tolerance of the lens.

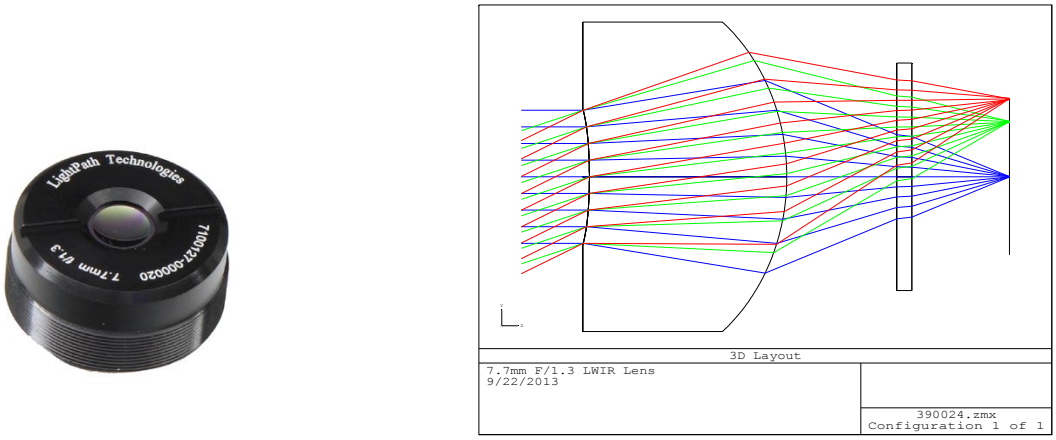

Figure 6: Example of Single element 7.7 mm focal length, f1.3 and post molding optical model

The second lens evaluated was a dual element 19 mm, f1.1 thermal imaging lens as shown in figure 7. If we substitute the post molding index of refraction and maintain the same distance from the lens to the image plane, the focal plane of the lens is shifted 0.045 mm away from the lens and the MTF drops by 15%. A simple refocusing brings the MTF back to the initial values. Again, the amount of focal shift at this level is within the manufacturing tolerance of the lens, but is close to the point where an optical redesign may be required depending on the final performance requirements of the lens.

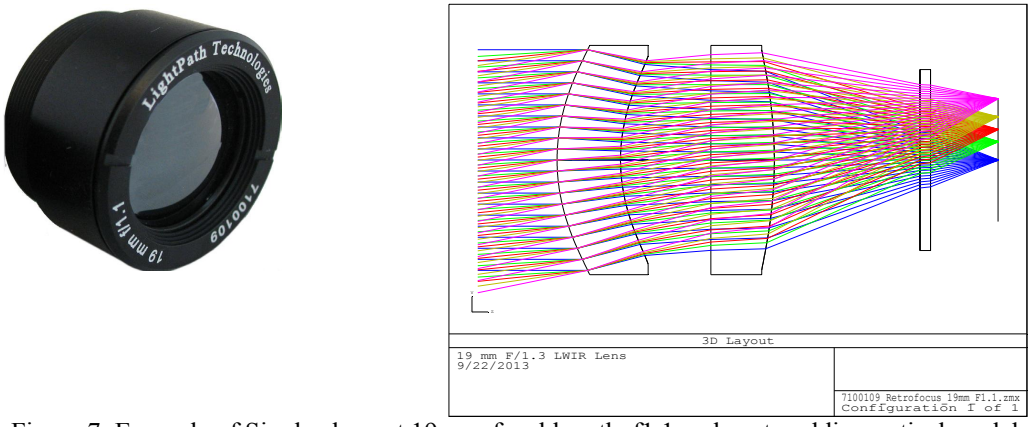

Figure 7: Example of Single element 19 mm focal length, f1.1 and post molding optical model

4. CONCLUSIONS

This study has shown that the indices of refraction of chalcogenide glasses do change during the molding process. The cooling rate of the glass was shown to directly affect the index drop. The index shift is approximately -0.004 and -0.015 for $Ge_{28}Sb_{12}Se_{60}$ and $As_{40}Se_{60}$, respectively. For $Ge_{28}Sb_{12}Se_{60}$, the index drop may or may not need to be taken into consideration in the lens design depending on the application but, for $As_{40}Se_{60}$, the index drop definitively requires the lens to be designed based on the post-molding index.

ACKNOWLEDGEMENTS

The authors of this paper would like to thank Dennis Knowles, Lorna Fleming and the Infrared Development team at LightPath Technologies for their contributions to this paper. All figures courtesy of LightPath Technologies Inc.

REFERENCES

[1] Fotheringham, U., Baltes, A., Fischer, P., Höhn, P., Jedamzik, R., Schenk, C., Stolz, C., and Westenberger, G., "Refractive index drop observed after precision molding of optical elements: a quantitative understanding based on the Tool-Narayanaswamy-Moynihan model," *Journal of the American Ceramic Society*, Vol. 91, No. 3, pp. 780-783, 2008.

[2] Zhao, W., Chen, Y., Shen, L., and Yi, A.Y., "Refractive index and dispersion variation in precision optical glass molding by computed tomography," *Applied Optics*, Vol. 48, No. 19, pp. 3588-3595, 2009.

[3] Su, L., Chen, Y., Yi, A.Y., Klocke, F., and Pongs, G., "Refractive index variation in compression molding of precision glass optical components," *Applied Optics*, Vol. 47, No. 10, pp. 1662-1667, 2008.